Silk Functionalization

How to cite:
International Edition: doi.org/10.1002/anie.202015592
German Edition: doi.org/10.1002/ange.202015592

Functionalization of Silk by AIEgens through Facile Bioconjugation: Full-Color Fluorescence and Long-Term Bioimaging

Chenchen Liu, Haotian Bai, Benzhao He, Xuewen He, Jianyu Zhang, Chao Chen, Yanping Qiu, Rong Hu, Fangxin Zhao, Yunxiao Zhang, Wei He, Joe H. C. Chau, Sijie Chen, Jacky W. Y. Lam, and Ben Zhong Tang**

Abstract: *Silkworm silk is a promising natural biopolymer for textile and biomedical applications for its remarkable flexibility, excellent biocompatibility and controllable biodegradability. The functionalization of silks makes them more versatile for flexible displays and visible bioscaffolds. However, fluorescent silks are normally fabricated through unstable physical absorption or complicated chemical reactions under harsh conditions. Herein, we developed a simple strategy for preparing fluorescent silks. Five aggregation-induced emission luminogens (AIEgens) with activated alkynes were synthesized by rational molecular design, and then reacted with silk fibers through facile metal-free click bioconjugation. The resulting conjugates show bright full-color emissions and high stability. A white light-emitting silk was fabricated by simultaneous bioconjugation with red-, green- and blue-emissive AIEgens. The red-emissive AIEgen-functionalized silks were successfully applied for long-term cell tracking and two-photon bioimaging, demonstrating great potential for tissue engineering and bioscaffold monitoring.*

Introduction

Natural biopolymers have been widely utilized in biomedical areas with good biocompatibility and biodegradability, and are accessible from abundant natural sources. For example, polysaccharides like cellulose and chitosan could be obtained directly from trees and crab shells, but need complicated preparation procedures in the presence of harsh chemical treatment for their synthesis in the laboratory.[1] As a unique natural fibrous protein, silkworm silk can be easily prepared from cocoon and has been used for textile applications historically with excellent physical properties, such as flexibility, luster smoothness, light weight and high mechanical strength. Recently, the remarkable biocompatibility and controllable biodegradability of silk make it favorable as the structural material in tissue engineering.[2] Additionally, silk can be functionalized to show advanced properties such as fluorescence, stimulus and conductivity, making them more attractive for flexible display, electronic skin and bioimaging applications.[3]

Fluorescent silk materials exhibit great advantages in functional bio-optical devices[4] and bio-scaffolds.[5] Thus, it is urgent to explore high performance fluorescent dyes and efficient dyeing procedures for silk functionalization. However, conventional dyeing procedures require harsh conditions like high temperature and low pH,[6] which consume much energy and may damage the protein structures of silk. In addition, many fluorescent silk materials were fabricated by physical absorption through hydrogen bonding or electrostatic attraction. For example, fluorescent silk proteins can be modified with inorganic quantum dots (QDs) through hydrogen bond.[7] However, such non-covalent interaction is unstable in physiological environment to result in easy leakage of inorganic QDs that may cause harm to health.[8] In addition, many organic fluorescent dyes suffer from the aggregation-caused quenching (ACQ) effect in the aggregate state due to the strong π-π stacking, they have to be molecularly dissolved to avoid the ACQ effect for silk functionalization.[9] Therefore, chemical modification of silk with solid-state emissive fluorophores seems to be the best approach to fabricate bright and stable fluorescent silk. However, there still remains many challenges and difficulties which restrict the development of silk functionalization.

[*] C. Liu, Dr. H. Bai, Dr. B. He, Dr. X. He, J. Zhang, Dr. C. Chen, W. He, J. H. C. Chau, Dr. J. W. Y. Lam, Prof. B. Z. Tang
Department of Chemistry, Hong Kong Branch of Chinese National Engineering Research Center for Tissue Restoration and Reconstruction, Division of Life Science and State Key Laboratory of Molecular Neuroscience, Institute for Advanced Study and Department of Chemical and Biomedical Engineering, The Hong Kong University of Science and Technology
Clear Water Bay, Kowloon, Hong Kong (China)
E-mail: tangbenz@ust.hk

Y. Qiu, Dr. R. Hu, Prof. B. Z. Tang
Center for Aggregation-Induced Emission, SCUT-HKUST Joint Research Institute, State Key Laboratory of Luminescent Materials and Devices, South China University of Technology
Guangzhou 510640 (China)

F. Zhao
Department of Ocean Science, The Hong Kong University of Science and Technology
Clear Water Bay, Kowloon, Hong Kong (China)

Y. Zhang
Department of Mechanical and Aerospace Engineering, The Hong Kong University of Science and Technology
Clear Water Bay, Kowloon, Hong Kong (China)

Prof. S. Chen, Prof. B. Z. Tang
Ming Wai Lau Centre for Reparative Medicine, Karolinska Institute
Sha Tin, Hong Kong (China)

Supporting information and the ORCID identification number(s) for the author(s) of this article can be found under: https://doi.org/10.1002/anie.202015592.

These are not the final page numbers!

In contrast to traditional ACQ dyes, aggregation-induced emission luminogens (AIEgens) exhibit intense emission in the solid state due to the restriction of molecular motion. For example, tetraphenylethylene (TPE) is a typical AIE molecule that is not emissive in the solution state, because the energy is dissipated from non-radiative excited-state decay. However, it can exhibit intense emission in the aggregation state due to the restriction of molecular motion. In addition, the modification of traditional ACQ dyes with AIE units is an efficient method to design new AIE molecules, which are inherently suitable for fabricating solid-state luminescent devices like organic light-emitting diodes.[10] Actually, AIEgens have already been successfully applied for the functionalization of silk materials for flexible display and biomedical application.[11] Undoubtedly, AIEgens are remarkable candidates for fabricating bright and stable fluorescent silks through bioconjugation. However, the well-known azide-alkyne cycloaddition or the so called "click" reaction requires the use of copper catalyst which may quench the fluorescence and cause damage to health. And prefunctionalization of the silk proteins makes the dyeing process more complicated.[12] Recently, our group developed a simple strategy for metal-free "click" bioconjugation based on activated alkynes for protein modification, which is promising for silk functionalization.[13] Inspired by the inherent bright emission of AIEgens in the solid state and the facile bioconjugation process, in this work we synthesized full-color emissive AIEgens with activated alkynes by rational molecular design, for the purpose of fabricating chemical conjugated fluorescent silk with bright emission and great stability. As a proof of concept, a flexible white light-emitting silk was fabricated by simultaneous bioconjugation of red-, green- and blue- emissive AIEgens. In addition, AIEgen-functionalized silk with red emission manifested great potential for long-term cell tracking and two-photon bioimaging.

Results and Discussion

Five AIE molecules with propynone groups (AIE-pyo) and emission color covering the whole visible region (blue, green, yellow, orange and red) were designed and synthesized (Figure 1a). TPE is a typical AIEgen that emits blue fluorescence under UV irradiation, so TPE was functionalized with propynone group to design blue-emissive AIE-pyo luminogen according to the reported method (Scheme S1).[13a] Then, methoxy and benzothiadiazole groups were selected as the electron-donating and electron-withdrawing groups, respectively. They were introduced to synthesize MTPEP-pyo, TPEBP-pyo and MTPEBP-pyo with D-A structures and longer-wavelength emissions (Scheme S2–S4). Triphenylamine (TPA) was widely utilized as the electron-donating group and molecular rotor to build new AIEgens, therefore stronger electron-donating methoxytriphenylamine (MTPA) group was chosen to synthesize MTPABP-pyo with red emission (Scheme S5). The intermediates and products were carefully characterized by ^{1}H NMR, ^{13}C NMR and MS spectra with satisfactory results (Supporting Information). For example, the FT-IR spectra of AIE-pyo definitely confirmed the existence of alkyne groups (C≡C stretching at $\approx 2160\ cm^{-1}$) and ketone groups (C=O stretching at $\approx 1680\ cm^{-1}$) (Figure S1).

The absorption spectra of AIE-pyo luminogens were first measured and the absorption maximum red-shifted from ultraviolet to visible spectral region with increasing D-A interaction (Figure 1b). Then we evaluated the AIE property of TPE-pyo. TPE-pyo showed weak emission in DMSO solution due to the free rotation of the phenol rings that facilitates the non-radiative excited-state decay.[10a] After addition of a poor solvent of water into its DMSO solution, the molecular motion could be largely restricted to result in remarkable enhancement of fluorescent emission (Figure 1c). Other AIE-pyo luminogens also manifested similar AIE

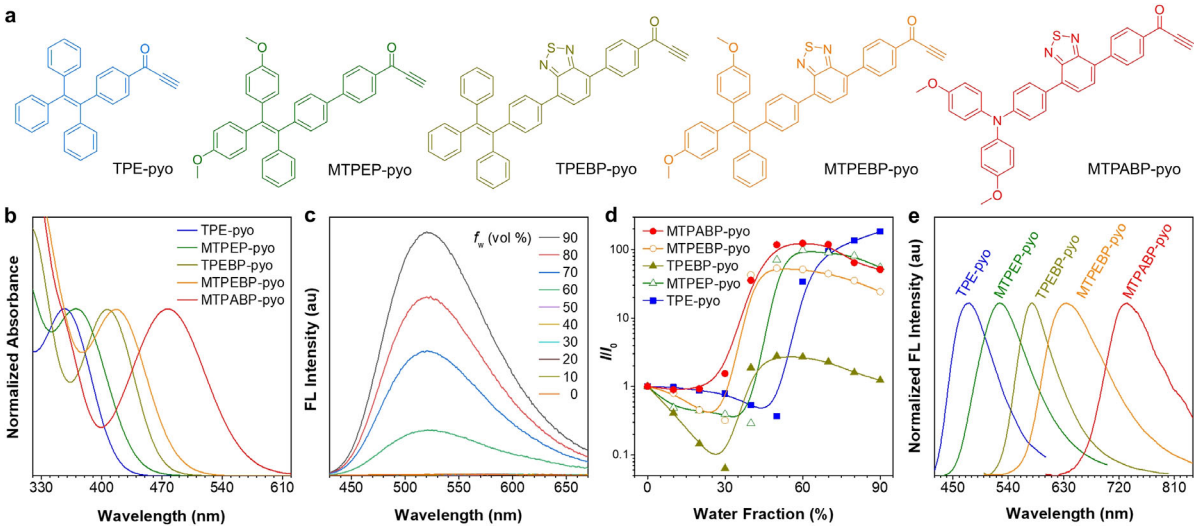

Figure 1. a) Molecular structures of AIE-pyo luminogens. b) Normalized absorption spectra of AIE-pyo luminogens in DMSO solutions. c) Fluorescence spectra of TPE-pyo (10^{-5} M) in DMSO/H_2O mixtures with different fractions of water (f_w). d) Plots of relative fluorescence intensity (I/I_0) of AIE-pyo luminogens versus the composition of their DMSO/H_2O mixtures. e) Normalized fluorescence spectra of AIE-pyo luminogens in the solid state.

behaviors (Figure 1d and Figure S2). Among them, TPEBP-pyo exhibited obvious twisted intramolecular charge transfer (TICT) effect and its emission was weakened and red-shifted gradually in solvents with increasing polarity. However, when aggregates formed, the emission became stronger again with a slight blue-shift owing to the comparatively lower polar environment inside the nanoparticles (Figure S2d). Full-color emissions were realized by rationally tuning the D-A structures of the AIE-pyo luminogens (Figure 1e). Theoretical calculation confirmed the efficient separation of HOMO and LUMO in molecules with strong D-A interaction, which resulted in decreased energy gaps and red-shifted absorption and emissions. (Figure S3)

The efficient metal-free "click" bioconjugation of activated alkynes with amine groups was previously reported, and showed great potential for facile functionalization of biomaterials.[13] As a proof of concept, the model metal-free "click" reaction was evaluated between n-butylamine and five AIE-pyo luminogens, the spontaneous reaction finished within 30 minutes at room temperature and molecular structures of the products were successfully characterized by ^{1}H-NMR, ^{13}C-NMR and HRMS analysis (Scheme S6). In addition, native bovine serum albumin (BSA) and MTPABP-pyo were taken as examples to evaluate the feasibility of amino-yne click bioconjugation (Figure 2). BSA consists of 59 lysine residues and 30–35 of them have primary amines that are capable of reacting with activated alkynes.[13a,14] As shown in Figure 2a, one primary amine group of BSA was taken to demonstrate the metal-free "click" bioconjugation process, which could be readily occurred by stirring a mixture of BSA and MTPABP-pyo in aqueous solution at room temperature. The formation of fluorescent MTPABP-BSA bioconjugates was successfully verified by sodium dodecyl sulfate polyacrylamide gel electrophoresis, where the MTPABP-labelled BSA exhibited bright fluorescence under UV irradiation (Figure 2b). Therefore, AIE-pyo luminogens manifested great potential for silk functionalization.

As there are many primary amine groups in the lysine residues of silk proteins, they can be employed for facile bioconjugation with activated alkyne groups.[15] Thus, AIE-pyo functionalized silks (AIEgen-silks) were conveniently fabricated by immersing silk fibers into AIE-pyo solutions at room temperature overnight, and AIEgen-silk threads and fabrics with uniform fluorescence covering the entire visible light region were obtained (Figure 3 and Table S1). Next, the

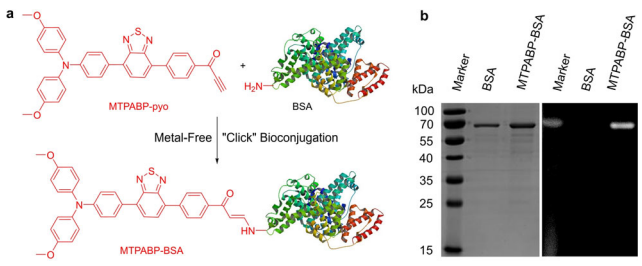

Figure 2. a) Metal-free "click" reaction of MTPABP-pyo with native BSA without prefunctionalization at room temperature. b) Verification of bioconjugation between MTPABP-pyo and BSA by SDS-PAGE separation: (left) bright field and (right) fluorescent image.

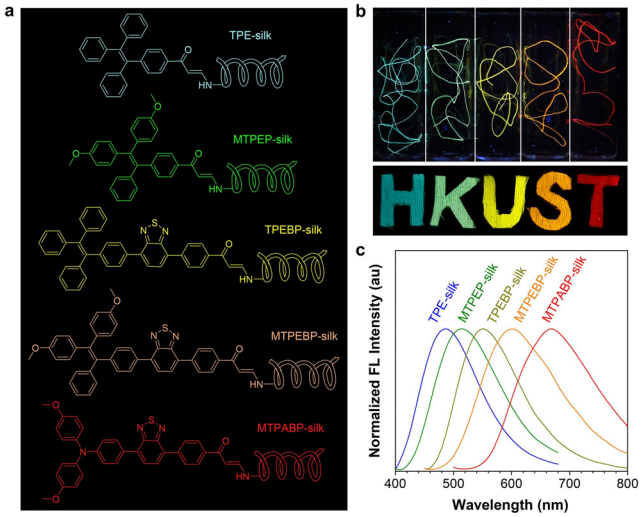

Figure 3. a) AIEgen-silk bioconjugates with full-color emissions in the visible spectral region. b) Fluorescent photos of (upper) threads and (lower) fabrics of AIEgen-silks taken under 365 nm UV light illumination. c) Normalized fluorescence spectra of AIEgen-silk fabrics.

mechanical properties of the AIEgen-silk threads were compared with the untreated ones and no obvious difference was observed (Figure S5). This meant that the bioconjugation process did not affect the mechanical properties of natural silk.

To demonstrate the advantages of AIE-pyo over traditional fluorescent dyes in silk functionalization, fluorescein was chosen for comparison. First, as a typical ACQ fluorophore, fluorescein showed strong fluorescence in solution, but much weakened emission in the solid state due to strong π-π interaction (Figure 4c and Table S2). Actually, the ACQ effect has limited the solid-state applications of many fluorophores including silk functionalization.[9] Thus, ACQ

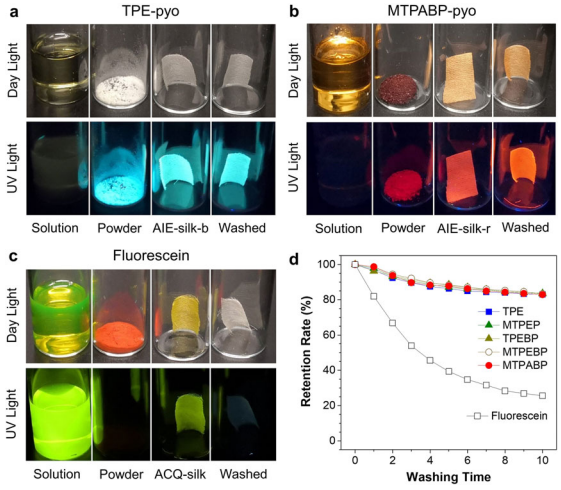

Figure 4. Photos of a) TPE-pyo, b) MTPABP-pyo and c) fluorescein in solution and powdery states, and dye-modified silk fabrics before and after washing (with soapy water for 10 times) taken under (upper) room lighting and (lower) UV illumination. d) Variation of dyes retained on the silk fabrics after repeated washing.

dyes like fluorescein should be dispersed molecularly in silk fibers, which is hard to control and unstable for long-term usage. Consequently, AIE luminogens with intense solid-state emissions manifested inherent advantages in fabricating fluorescent silk. Next, fluorescein-silk was fabricated through hydrogen bond interaction, and its stability was evaluated and compared with chemically conjugated AIEgen-silks. The blue AIEgen-silk (AIE-silk-b) and red AIEgen-silk (AIE-silk-r) fabrics exhibited intense emission even after ultrasonic cleaning with soapy water for ten times (Figure 4a,b). In contrast, although fluorescein modified-silk exhibited yellow fluorescence due to the partial segregation of the fluorescein molecules by silk polymeric chains, its fluorescence was reduced dramatically after soap washing for ten times due to the unstable physical interaction (Figure 4c). Obviously, the retention rates of AIEgens on silk fabrics were much higher than that of fluorescein, in corresponding to higher stability contributed by chemical bonding than physical absorption (Figure 4d and Figure S6). Owing to inherent solid-state emission and stable covalent bonding, AIE-pyo luminogens exhibited great advantages in fabricating fluorescent silks with high brightness and high stability.

White light-emitting (WLE) materials and devices have attracted considerable attention in lighting and displays. In principle WLE could be achieved by mixing three primary RGB colors (red, green and blue).[7,16] Thus, WLE silk was fabricated through simultaneous bioconjugation with blue-, green- and red-emissive AIE-pyo luminogens at a precisely controlled molar ratio of 88:6:6, with a CIE coordinate of (0.33, 0.36) (Figure 5a,b). The fluorescence resonance energy transfer occurred due to the overlapping of absorption of red AIEgen with the fluorescence of blue and green AIEgens (Figure S7). Notably, WLE silk fibers of different shapes were easily fabricated with excellent flexibility, demonstrating potential applications in flexible displays and wearable electronic devices (Figure 5c).

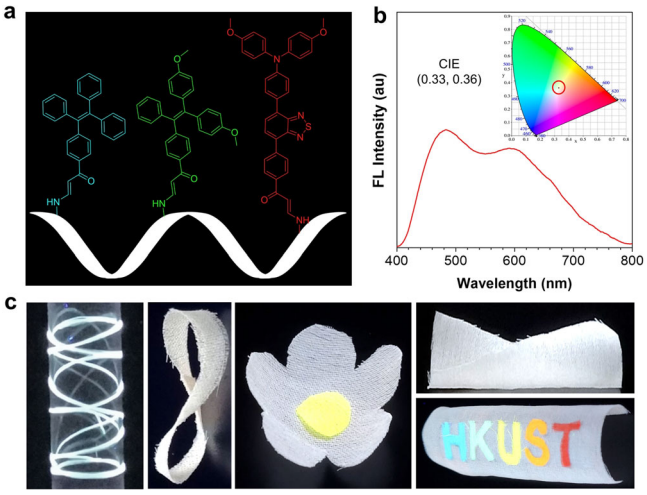

Figure 5. a) Preparation of white light-emitting (WLE) silk through bioconjugation with TPE-pyo, MTPEP-pyo and MTPABP-pyo at a molar ratio of 88:6:6. b) Fluorescence spectrum of the WLE silk fabric and (insert) its CIE coordinate. c) Fluorescence photos of flexible WLE fabrics fabricated from the AIEgen-silk fibers.

Due to the remarkable biocombability and controllable degradability, functionalized silks have been successfully utilized for tissue engineering scaffolds.[5] In addition, red and near infrared-emissive AIEgens play important roles in bioimaging with high penetration depth and low tissue autofluorescence.[17] Therefore, we attempted to fabricate red-emissive silk materials through bioconjugation of hydrolyzed silk protein with red-emissive MTPABP-pyo. The hydrodynamic size distribution of MTPABP-hydrolyzed silk in 1% DMSO aqueous solution was evaluated and the average diameter is 26.8 nm (Figure S8). Both hydrolyzed silk and MTPABP-functionalized hydrolyzed silk showed excellent biocombability on A549 cells even at a high concentration of 125 $\mu g\,mL^{-1}$ (Figure 6a,b). Next, one-photon cell imaging study was evaluated by staining the A549 cells with red-emissive MTPABP-functionalized hydrolyzed silk. As indicated in Figure 6c, the plasma membrane could be visualized clearly with excellent image contrast within 2 min, attributed to the remarkable cell attachment ability of the silk protein.[18] Then, the dye gradually entered the cells with increased emission intensity within 2 h, showing an entire cellular uptake process. Moreover, we continued to monitor the cell growth for different passages by confocal imaging (Figure 7). Although the concentration of MTPABP-functionalized hydrolyzed silk in cells gradually decreased during the process of cell division, red emission could still be clearly observed for up to 11 days, which demonstrated the great potential of AIE-silk bioconjugates for long-term cell tracking.

Recently, two-photon fluorescence (2PF) imaging has attracted much attention in deep-tissue imaging due to its great advantages such as low tissue autofluorescence, long-wavelength excitation and high spatiotemporal resolution.[19] Materials with large two-photon absorption (2PA) cross-section (σ_{2PA}) are found to show enhanced 2PF imaging performance, and the introduction of strong electron donor and acceptor groups is an efficient strategy to increase the σ_{2PA} value.[20] The σ_{2PA} values of the AIE-pyo luminogens were measured by two-photon-induced fluorescence experiments. As shown in Figure 8a, the σ_{2PA} values increased in accordance with the extent of D-A interaction and among them, the red-emissive MTPABP-pyo showed the highest σ_{2PA} value of up to 190 GM under 920 nm excitation. Therefore, the MTPABP-functionalized silk fabrics were chosen for further two-photon imaging experiments. First, the fine morphology of MTPABP-functionalized silk fabric was clearly visualized under two-photon excitation, manifesting much better spatiotemporal resolution than one-photon excitation (Figure S9a). In addition, the three-dimensional (3D) structure of the silk fabric with a thickness of 160 μm could be precisely reconstructed from top to bottom by 2PF imaging (Figure S9b). On the other hand, the noninvasive real-time monitoring of bioscaffold is of great importance in drug delivery and tissue engineering. Encouraged by the high penetration depth of 2PF imaging, we further evaluated the MTPABP-functionalized silk fabric for deep-tissue imaging and bioscaffold monitoring. Chicken breast tissues were selected to mimic the optical diffusion in biological systems. As shown in Figure 8b, the structure of the silk fabrics was

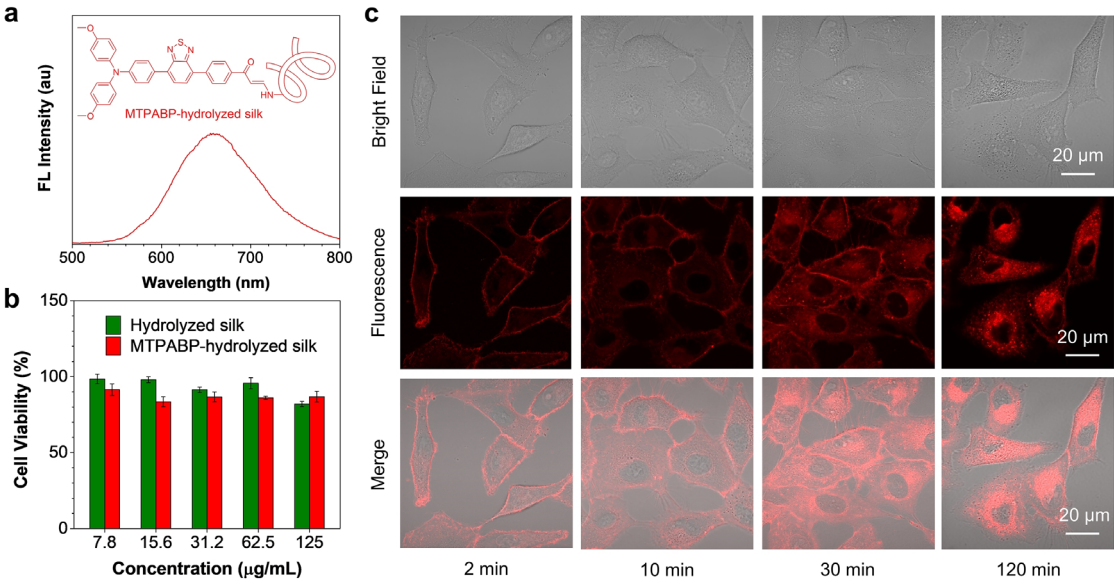

Figure 6. a) Fluorescence spectrum of hydrolyzed silk conjugated with MTPABP-pyo. b) Biocompatibility of the hydrolyzed silk and its AIEgen-conjugate. c) Staining of A549 cells with MTPABP-functionalized hydrolyzed silk (100 $\mu g\,mL^{-1}$); fluorescent images taken at $\lambda_{ex} = 488$ nm and $\lambda_{em} = 565–700$ nm.

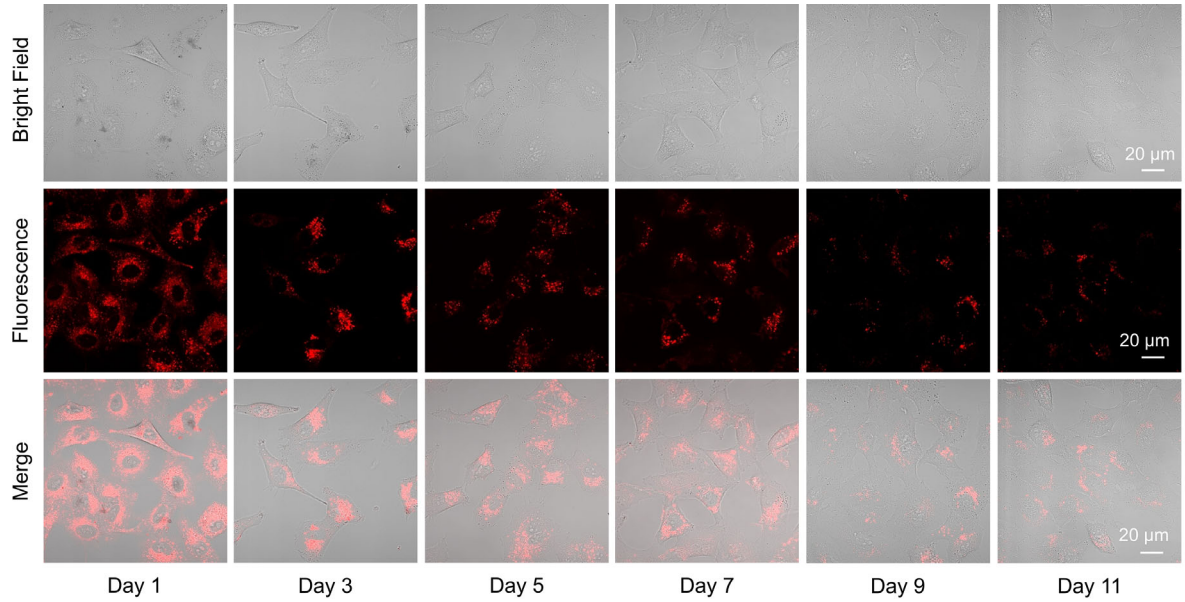

Figure 7. Long-term tracking of A549 cells by MTPABP-functionalized hydrolyzed silk; fluorescent images taken at $\lambda_{ex} = 488$ nm and $\lambda_{em} = 565–700$ nm.

clearly visualized even the fabrics were covered by chicken tissues. The red emission could penetrate through a thickness of up to 1200 μm. Such a result demonstrated the great possibility of the present bioconjugate for monitoring the silk bioscaffold in real physiological systems.

Conclusion

In summary, we developed a simple strategy for silk functionalization by AIEgens through facile metal-free click bioconjugation. The chemically conjugated fluorescent silks exhibited great stability and realized full-color emissions by rational molecular design. A white light-emitting silk was achieved by simultaneous bioconjugation with red-, green- and blue-emissive AIEgens. Additionally, red emissive MTPABP-functionalized hydrolyzed silk was successfully applied for real-time and long-term cell tracking. MTPABP-functionalized silk fabrics showed large two-photon absorption and demonstrated great potential for deep-tissue imaging and bioscaffold monitoring. It is believed that the facile bioconjugation strategy developed in the present work will inspire the development of functionalized silk materials with

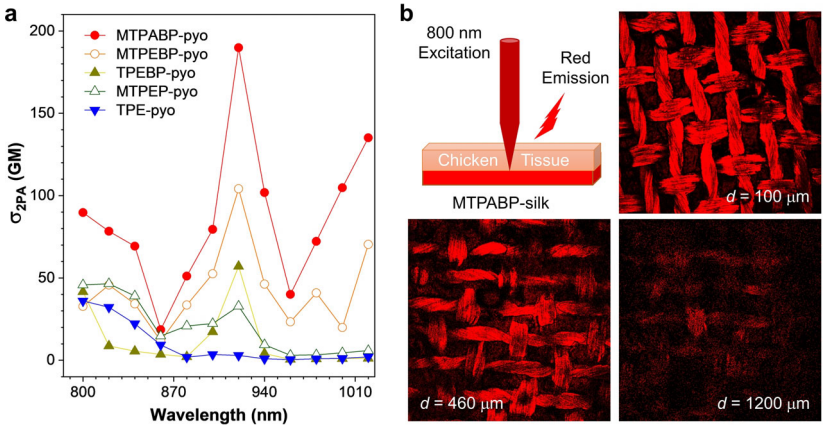

Figure 8. a) Two-photon absorption cross-sections of AIE-pyo luminogens. b) Two-photon fluorescent images of MTPABP-functionalized silk fabrics covered by chicken tissues with thickness (*d*) of 100, 460 and 1200 μm; photos taken at λ_{ex} = 800 nm and λ_{em} = 650–750 nm.

photodynamic or photothermal properties for promising tissue engineering and therapeutic applications.

Acknowledgements

We are grateful for financial support from the National Science Foundation of China (21788102), the Research Grants Council of Hong Kong (16305618, 16304819, N_HKUT609/19 and C6009-17G), the Innovation and Technology Commission (ITC-CNERC14SC01 and ITCPD/17-9), the Science and Technology Plan of Shenzhen (JCYJ20170818113602462 and JCYJ20180507183832744), and the Ming Wai Lau Centre for Reparative Medicine Associate Member Programme (MWLC11SC2021).

Conflict of interest

The authors declare no conflict of interest.

Keywords: aggregation-induced emission · flexible display · long-term cell tracking · silk functionalization · two-photon emission

[1] a) H. Wang, G. Gurau, R. D. Rogers, *Chem. Soc. Rev.* **2012**, *41*, 1519–1537; b) A. Farrán, C. Cai, M. Sandoval, Y. Xu, J. Liu, M. J. Hernaiz, R. J. Linhardt, *Chem. Rev.* **2015**, *115*, 6811–6853.
[2] N. Lin, L. Cao, Q. Huang, C. Wang, Y. Wang, J. Zhou, X.-Y. Liu, *Adv. Funct. Mater.* **2016**, *26*, 8885–8902.
[3] a) W. Huang, S. Ling, C. Li, F. G. Omenetto, D. L. Kaplan, *Chem. Soc. Rev.* **2018**, *47*, 6486–6504; b) N. C. Tansil, L. D. Koh, M. Y. Han, *Adv. Mater.* **2012**, *24*, 1388–1397.
[4] a) N. E. Kurland, T. Dey, C. Wang, S. C. Kundu, V. K. Yadavalli, *Adv. Mater.* **2014**, *26*, 4431–4437; b) J. P. Mondia, J. J. Amsden, D. Lin, L. D. Negro, D. L. Kaplan, F. G. Omenetto, *Adv. Mater.* **2010**, *22*, 4596–4599; c) S. T. Parker, P. Domachuk, J. Amsden, J. Bressner, J. A. Lewis, D. L. Kaplan, F. G. Omenetto, *Adv. Mater.* **2009**, *21*, 2411–2415.
[5] a) N. Lin, G. W. Toh, Y. Feng, X. Y. Liu, H. Xu, *J. Mater. Chem. B* **2014**, *2*, 2136–2143; b) M. Amirikia, S. M. A. Shariatzadeh, S. G. A. Jorsaraei, M. S. Mehranjani, *Eur. Biophys. J.* **2018**, *47*, 573–581; c) D. W. Kim, O. J. Lee, S. W. Kim, C. S. Ki, J. R. Chao, H. Yoo, S. I. Yoon, J. E. Lee, Y. R. Park, H. Kweon, K. G. Lee, D. L. Kaplan, C. H. Park, *Biomaterials* **2015**, *70*, 48–56; d) L. Cheng, H. Zhao, H. Huang, B. Li, R. K. Y. Li, X.-Q. Feng, F. Dai, *J. Mater. Sci.* **2019**, *54*, 9945–9957; e) Z. Z. Zheng, M. Liu, S. Z. Guo, J. B. Wu, D. S. Lu, G. Li, S. S. Liu, X. Q. Wang, D. L. Kaplan, *J. Mater. Chem. B* **2015**, *3*, 6509–6519; f) N. C. Tansil, Y. Li, C. P. Teng, S. Zhang, K. Y. Win, X. Chen, X. Y. Liu, M. Y. Han, *Adv. Mater.* **2011**, *23*, 1463–1466.
[6] a) M. L. Gulrajani, *Rev. Prog. Color. Relat. Top.* **1993**, *23*, 51–56; b) Y. Zhou, J. Zhang, R.-C. Tang, J. Zhang, *Ind. Crops Prod.* **2015**, *64*, 224–232.
[7] N. Lin, F. Hu, Y. Sun, C. Wu, H. Xu, X. Y. Liu, *Adv. Funct. Mater.* **2014**, *24*, 5284–5290.
[8] A. Valizadeh, H. Mikaeili, M. Samiei, S. M. Farkhani, N. Zarghami, M. Kouhi, A. Akbarzadeh, S. Davaran, *Nanoscale Res. Lett.* **2012**, *7*, 480.
[9] N. Lin, X. Y. Liu, Y. Y. Diao, H. Xu, C. Chen, X. Ouyang, H. Yang, W. Ji, *Adv. Funct. Mater.* **2012**, *22*, 361–368.
[10] a) J. Mei, N. L. Leung, R. T. Kwok, J. W. Lam, B. Z. Tang, *Chem. Rev.* **2015**, *115*, 11718–11940; b) H. Wang, E. Zhao, J. W. Y. Lam, B. Z. Tang, *Mater. Today* **2015**, *18*, 365–377.
[11] a) G. Zhang, R. Wang, L. Shi, C. Zhang, Y. Zhang, Y. Zhou, C. Dong, G. Li, S. Shuang, *Sens. Actuators B* **2019**, *279*, 361–368; b) Q. Zhan, S. Fan, D. Wang, X. Yao, H. Shao, Y. Zhang, *Compos. Commun.* **2020**, *21*, 100414.
[12] V. V. Rostovtsev, L.G. Green, V. V. Fokin, K. B. Sharpless, *Angew. Chem. Int. Ed.* **2002**, *41*, 2596–2599; *Angew. Chem.* **2002**, *114*, 2708–2711.
[13] a) X. Hu, X. Zhao, B. He, Z. Zhao, Z. Zheng, P. Zhang, X. Shi, R. T. K. Kwok, J. W. Y. Lam, A. Qin, B. Z. Tang, *Research* **2018**, *2018*, 3152870; b) Y. Zhang, J. Shen, R. Hu, X. Shi, X. Hu, B. He, A. Qin, B. Z. Tang, *Chem. Sci.* **2020**, *11*, 3931–3935; c) H. Liu, L. H. Xiong, R. T. K. Kwok, X. He, J. W. Y. Lam, B. Z. Tang, *Adv. Opt. Mater.* **2020**, *8*, 2000162; d) B. He, H. Su, T. Bai, Y. Wu, S. Li, M. Gao, R. Hu, Z. Zhao, A. Qin, J. Ling, B. Z. Tang, *J. Am. Chem. Soc.* **2017**, *139*, 5437–5443.
[14] a) M. M. Mir, K. M. Fazili, M. A. Qasim, *Biochim. Biophys. Acta Protein Struct. Mol. Enzymol.* **1992**, *1119*, 261–267; b) K. A. Majorek, P. J. Porebski, A. Dayal, M. D. Zimmerman, K. Jablonska, A. J. Stewart, M. Chruszcz, W. Minor, *Mol. Immunol.* **2012**, *52*, 174–182.
[15] T. Gamo, *JARQ* **1987**, *21*, 53–58.
[16] a) Q. W. Zhang, D. Li, X. Li, P. B. White, J. Mecinovic, X. Ma, H. Agren, R. J. M. Nolte, H. Tian, *J. Am. Chem. Soc.* **2016**, *138*, 13541–13550; b) G. Naren, C. W. Hsu, S. Li, M. Morimoto, S. Tang, J. Hernando, G. Guirado, M. Irie, F. M. Raymo, H. Sunden, J. Andreasson, *Nat. Commun.* **2019**, *10*, 3996; c) W. Tian, J. Zhang, J. Yu, J. Wu, J. Zhang, J. He, F. Wang, *Adv. Funct. Mater.* **2018**, *28*, 1793548.
[17] R. Zhang, Y. Duan, B. Liu, *Nanoscale* **2019**, *11*, 19241–19250.
[18] N. Minoura, S. Aiba, M. Higuchi, Y. Gotoh, M. Tsukada, Y. Imai, *Biochem. Biophys. Res. Commun.* **1995**, *208*, 511–516.
[19] a) Y. Gao, G. Feng, T. Jiang, C. Goh, L. Ng, B. Liu, B. Li, L. Yang, J. Hua, H. Tian, *Adv. Funct. Mater.* **2015**, *25*, 2857–2866; b) X. Lou, Z. Zhao, B. Z. Tang, *Small* **2016**, *12*, 6430–6450; c) Z. Zheng, T. Zhang, H. Liu, Y. Chen, R. T. K. Kwok, C. Ma, P. Zhang, H. H. Y. Sung, I. D. Williams, J. W. Y. Lam, K. S. Wong,

B. Z. Tang, *ACS Nano* **2018**, *12*, 8145 – 8159; d) J. Yang, Y. Gao, T. Jiang, W. Liu, C. Liu, N. Lu, B. Li, J. Mei, Q. Peng, J. Hua, *Mater. Chem. Front.* **2017**, *1*, 1396 – 1405.

[20] M. Pawlicki, H. A. Collins, R. G. Denning, H. L. Anderson, *Angew. Chem. Int. Ed.* **2009**, *48*, 3244 – 3266; *Angew. Chem.* **2009**, *121*, 3292 – 3316.

Manuscript received: November 23, 2020
Revised manuscript received: March 18, 2021
Accepted manuscript online: March 24, 2021
Version of record online: ■■ ■■, ■■■■

Research Articles

Silk Functionalization

C. Liu, H. Bai,* B. He, X. He, J. Zhang, C. Chen, Y. Qiu, R. Hu, F. Zhao, Y. Zhang, W. He, J. H. C. Chau, S. Chen, J. W. Y. Lam, B. Z. Tang* ____ ▮▮▮▮–▮▮▮▮

Functionalization of Silk by AIEgens through Facile Bioconjugation: Full-Color Fluorescence and Long-Term Bioimaging

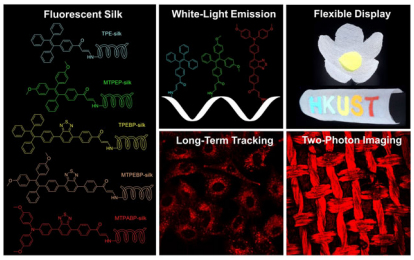

Fluorescent silks with full-color emissions were fabricated through facile metal-free click bioconjugation with five aggregation-induced emission luminogens (AIEgens). White light-emitting silk was prepared and demonstrated potential applications in flexible displays. Moreover, red-emissive AIEgen-functionalized silk materials were successfully applied for long-term cell tracking and two-photon bioimaging.